

Time-dependent thermoelectric transport in mesoscopic systems under a quantum quenchZhizhou Yu,¹ Jiangtao Yuan,² and Jian Wang^{2,*}¹*Center for Quantum Transport and Thermal Energy Science, School of Physics and Technology, Nanjing Normal University, Nanjing 210023, China*²*Department of Physics and HKU-UCAS Joint Institute for Theoretical and Computational Physics at Hong Kong, The University of Hong Kong, Hong Kong, China*

(Received 23 January 2020; revised manuscript received 31 March 2020; accepted 4 June 2020; published 19 June 2020)

We investigate the transient behavior of the quantum transport in mesoscopic systems under a quantum quench within the Caroli scheme. Using the nonequilibrium Green's function approach, an exact solution of the transient electric current, energy current, and their fluctuations in the presence of both external bias and temperature gradient are presented that goes beyond the wide-band limit. The exact solution of the time-dependent Seebeck coefficient in the linear response regime is also obtained. This formalism is applied to study the transient behavior of a single-level quantum dot with Lorentzian linewidth induced by the temperature gradient. The damped oscillatory behavior is found in the transient electric and energy currents, as well as their fluctuations. The oscillation frequency of electric and energy currents increases with the increasing energy level of quantum dot and the decay rate of oscillation decreases as the bandwidth increases. A significantly enhanced Seebeck coefficient is generated in the transient regime. We find the maximum value of the time-dependent Seebeck coefficient can be enhanced by increasing the energy level of the quantum dot and the reference temperature of leads.

DOI: [10.1103/PhysRevB.101.235433](https://doi.org/10.1103/PhysRevB.101.235433)**I. INTRODUCTION**

Over the past decades, with the rapid development of nanotechnology, substantial attention has been focused on electronic transport in nanodevices both theoretically and experimentally [1–3]. As the size of electronic devices shrinking down to the nanoscale, the heat dissipation due to high energy consumption becomes a critical problem. The thermoelectric effect, which describes a direct conversion from temperature gradient to electric voltage and vice versa, has received much attention due to its potential applications in harvesting the waste heat [4–7]. Recently, the static Seebeck coefficient was studied in various nanoscale structures such as carbon nanotubes and graphene-based molecular junctions [8–12]. In the linear response single-particle theory, the thermopower is related to the electronic conductance of nanodevices which can be simply modeled by the well-known Landauer-Büttiker formalism in dc transport [7,13,14]. Besides the static behavior, time-dependent thermoelectric transport is also an important issue that may provide fundamental insights to understand the thermal response of nanodevices.

In quantum transport, many different theoretical approaches are proposed to study the time-dependent response in quantum transport such as nonequilibrium Green's function (NEGF) [15–22], time-dependent density functional theory [23,24], quantum master equation [25,26], and coherent state

path integral method [27,28]. To model the nanoelectronic devices, a typical quantum transport system is the two-probe system in which the scattering region is connected to two semi-infinite leads. Generally, there are two different schemes to investigate the time-dependent quantum transport. One is the partition-free scheme (Cini scheme) in which the initial state of the system is assumed to be at equilibrium that can be described by a thermal density matrix [23,29]. Then the system can be perturbed by applying a time-dependent voltage bias. Recently, the time-dependent thermoelectric transport through the nanoscale devices including the transient energy and heat currents due to the bias and gate voltage was extensively studied using the NEGF method within the wide-band limit (WBL) based on the Cini scheme [19,30–33]. Another way to study the time-dependent quantum transport is the Caroli scheme which assumes that the two-probe system is disconnected initially and the coupling between the scattering region and two leads is treated as the time-dependent perturbation [34,35]. The dynamics of the Caroli scheme is also called quantum quench. By using the nonequilibrium Green's functions, it was shown that the formulas of current and lesser Green's function obtained by the Cini scheme and the Caroli scheme are equivalent [36,37].

In the study of thermoelectric transport, one needs to apply a temperature gradient between two leads. Since the concept of temperature was originally defined at the macroscopic level and varies slowly in space and time. It is difficult to encode the time-dependent temperature gradient into the initial density matrix to study the thermal transport at the nanoscale within the Cini scheme. The Luttinger-field approach

*jianwang@hku.hk

was proposed as a way to model the time-dependent temperature gradient within the WBL for transient transport calculations using the Cini scheme [38–40]. While within the Caroli scheme, the temperature gradient is applied in the remote past since the two-probe system is disconnected initially. The temperatures of both leads are time independent if the temperature distribution in the central region can be ignored. Therefore, it is essential to study the transient thermal transport within the Caroli scheme. Recently, the transient phonon transport in a nanoscale thermal switch was studied by abruptly turning on the coupling between leads [41,42]. The time-dependent thermoelectric transport was also studied through a gauge invariant theoretical framework which is similar to the Caroli scheme [43]. However, in time-dependent electric transport, less attention has been paid to the Caroli scheme. Furthermore, a theoretical formalism going beyond the WBL is necessary to investigate the transient behavior from first principles. Maciejko *et al.* derived an exact analytic solution of transient electric current within the Cini approach for a steplike pulse beyond the WBL [16]. However, the exact solution of electric and thermoelectric transport beyond the WBL is still absent for the Caroli scheme. It is the purpose of this paper to address these issues.

In this paper, the transient dynamics of thermoelectric transport are investigated within the Caroli scheme by using the NEGF method. The exact solution of transient electric current, energy current, and their corresponding fluctuations induced by both external bias and temperature gradient after a quantum quench is first presented beyond the WBL. Then this exact solution is used to obtain the time-dependent Seebeck coefficient in the linear response regime. Our formalism is applied to investigate the thermoelectric effect in the transient regime of a single quantum dot system. It is found that the transient electric and energy currents induced by the temperature gradient exhibit damped oscillatory behavior. The oscillation frequency of both electric and energy currents increases with the increasing energy level of quantum dot and the decay of oscillation amplitude becomes faster for the system with a larger bandwidth. The time-dependent fluctuations of electric and energy currents in the transient regime also exhibit similar oscillatory behavior. An enhanced thermopower is found in the transient regime and the maximum value of the time-dependent Seebeck coefficients can be tuned by both the energy level of quantum dot and the reference temperature.

The remainder of this paper is organized as follows. In Sec. II, the exact analytical solution of both transient electric and energy currents after a quantum quench are firstly derived. Then the exact solution of transient shot noise of electric and energy currents is given. The time-dependent thermopower is also presented in the linear response regime. This formalism is applied to a single-level quantum dot within the WBL and a single-level model with Lorentzian linewidth in which all Green's functions are solved exactly in the time domain. In Sec. III, the time-dependent electric current, energy current, fluctuations of electric and energy currents, and Seebeck coefficient of a single-level quantum dot are numerically investigated. Finally, a brief conclusion is given in Sec. IV.

II. THEORETICAL FORMALISM

A. Exact solution of electric and energy currents in the presence of both external bias and temperature gradient

The Hamiltonian of a general two-probe mesoscopic system can be written as

$$H = \sum_{k\alpha} \epsilon_{k\alpha} c_{k\alpha}^\dagger c_{k\alpha} + \sum_{mn} \epsilon_{mn} d_m^\dagger d_n + \sum_{k\alpha n} (t_{k\alpha n} c_{k\alpha}^\dagger d_n + \text{H.c.}), \quad (1)$$

where c_α^\dagger (c_α) and d_n^\dagger (d_n) are the creation (annihilation) operators of the electron on the lead α ($\alpha = L, R$) and the central region, respectively. $\epsilon_{k\alpha} = \epsilon_{k\alpha}^0 + qV_\alpha$ is the energy level in lead α in the presence of applied bias V_α with $\epsilon_{k\alpha}^0$ the bare energy level. ϵ_n is the energy level for the central region and $t_{k\alpha n}$ is the coupling constant between two leads and the central region. Within the Caroli scheme, it is assumed that the leads are at equilibrium states with the temperature T_α and applied bias V_α before $t = 0$ and the couplings between leads and the central region are turned on at $t = 0$.

The electric current $I_\alpha^0(t)$ and energy current $I_\alpha^1(t)$ of lead α are related to the time derivative of number operator $N_\alpha = \sum_k c_{k\alpha}^\dagger c_{k\alpha}$ and the lead Hamiltonian and are defined as $I_\alpha^0(t) = -\dot{N}_\alpha$ and $I_\alpha^1(t) = -\dot{H}_\alpha$, respectively. Applying the Heisenberg equation of motion, one obtains ($\hbar = e = 1$ for simplicity) [44,45],

$$I_\alpha^\chi(t) = -i \sum_{kn} \epsilon_{k\alpha}^\chi t_{k\alpha n} c_{k\alpha}^\dagger(t) d_n(t) + \text{H.c.} \quad (\chi = 0, 1). \quad (2)$$

After quantum and statistical average, the average electric and energy currents can be expressed in terms of NEGF [44,45],

$$I_\alpha^\chi(t) = \int_0^t dt_1 \text{Tr} [G^r(t, t_1) \Sigma_\alpha^{<, \chi}(t_1, t) + G^<(t, t_1) \Sigma_\alpha^{a, \chi}(t_1, t)] + \text{H.c.} \quad (\chi = 0, 1). \quad (3)$$

Here, $G^r(t_1, t_2)$ and $G^<(t_1, t_2)$ are the retarded Green's function and the lesser Green's function of the central region defined as $G_{mn}^r(t_1, t_2) = -i\theta(t_1 - t_2) \langle \{d_n(t_1), d_m^\dagger(t_2)\} \rangle$ and $G_{mn}^<(t_1, t_2) = i \langle d_m^\dagger(t_2) d_n(t_1) \rangle$, respectively. $\Sigma_\alpha^{\gamma, \chi}(t_1, t_2)$ ($\gamma = r, a, <$) is defined as [30,32]

$$\Sigma_{\alpha, mn}^{\gamma, \chi}(t_1, t_2) = \sum_k (\epsilon_{k\alpha})^\chi t_{k\alpha m}^* g_{k\alpha}^\gamma(t_1, t_2) t_{k\alpha n}, \quad (4)$$

where $g_{k\alpha}^\gamma(t_1, t_2)$ are the Green's functions of the isolated leads. After the Fourier transformation, $\Sigma_\alpha^{\gamma, \chi}(t_1, t_2)$ can be expressed as

$$\Sigma_\alpha^{\gamma, \chi}(t_1, t_2) = \int \frac{d\epsilon}{2\pi} \Sigma_\alpha^{\gamma, \chi}(\epsilon) e^{-i\epsilon(t_1 - t_2)}. \quad (5)$$

Here, $\Sigma_\alpha^{\gamma, \chi}(\epsilon) = \epsilon^\chi \Sigma_\alpha^\gamma(\epsilon)$ with $\Sigma_\alpha^\gamma(\epsilon)$ the self-energy due to the lead α in the energy domain. We note that the self-energy is only dependent on time difference since the bias is time independent at $t > 0$ within the Caroli scheme.

To calculate the electric and energy currents in Eq. (3), the key point is to solve the time-dependent Green's function. The retarded Green's function $G^r(t_1, t_2)$ satisfies the Dyson

equation [46],

$$G^r(t_1, t_2) = G_0^r(t_1, t_2) + \int_0^t dt_3 \int_0^t dt_4 G_0^r(t_1, t_3) \times \Sigma^r(t_3, t_4) G^r(t_4, t_2), \quad (6)$$

where $G_0^r(t_1, t_2)$ is the retarded Green's function of the isolated central region and $\Sigma^r = \sum_\alpha \Sigma_\alpha^r$. For the time-dependent transport behavior, instead of working directly with the retarded Green's function, we introduce the spectral function defined as

$$A(\epsilon, t) = \int_0^t dt' G^r(t, t') e^{i\epsilon(t-t')}. \quad (7)$$

By multiplying $\int_0^{t_1} dt_2 e^{i\epsilon(t_1-t_2)}$ on both sides of Eq. (6), the Dyson equation can be rewritten as

$$A(\epsilon, t) = \check{A}_0(\epsilon, t) + \int_0^t dt_1 \check{G}_0^r(t-t_1) \times \int_0^{t_1} dt_2 \check{\Sigma}^r(t_1-t_2) A(\epsilon, t_2), \quad (8)$$

where $\check{G}_0^r(t-t_1) = G_0^r(t-t_1) e^{i\epsilon(t-t_1)}$, $\check{\Sigma}^r(t_1-t_2) = \Sigma^r(t_1-t_2) e^{i\epsilon(t_1-t_2)}$, and $\check{A}_0(\epsilon, t) = \int_0^t dt' G_0^r(t-t') e^{i\epsilon(t-t')}$. After the Laplace transformation, Eq. (8) becomes

$$A(\epsilon, \sigma) = \check{A}(\epsilon, \sigma) + \check{G}_0^r(\epsilon, \sigma) \check{\Sigma}^r(\epsilon, \sigma) A(\epsilon, \sigma). \quad (9)$$

Here, $A(\epsilon, \sigma) = \int_0^\infty dt A(\epsilon, t) e^{-\sigma t}$ ($\text{Re } \sigma > 0$) and $\check{G}_0^r(\epsilon, \sigma)$ can be expressed in terms of the isolated retarded Green's function,

$$\check{G}_0^r(\epsilon, \sigma) = \int_0^\infty dt G_0^r(t) e^{i\epsilon t} e^{-\sigma t} = G_0^r(\epsilon + i\sigma). \quad (10)$$

Similarly, we can obtain $\check{\Sigma}_0^r(\epsilon, \sigma) = \Sigma^r(\epsilon + i\sigma)$ and $\check{A}(\epsilon, \sigma) = \frac{1}{\sigma} G_0^r(\epsilon + i\sigma)$. Then the spectral function $A(\epsilon, \sigma)$ can be written as

$$\begin{aligned} A(\epsilon, \sigma) &= [1 - \check{G}_0^r(\epsilon, \sigma) \check{\Sigma}^r(\epsilon, \sigma)]^{-1} \check{A}(\epsilon, \sigma) \\ &= \frac{1}{\sigma} [1 - G_0^r(\epsilon + i\sigma) \Sigma^r(\epsilon + i\sigma)]^{-1} G_0^r(\epsilon + i\sigma). \end{aligned} \quad (11)$$

In the steady state when $t = \infty$, it is well known that the retarded Green's function $G^r(\epsilon)$ satisfies the following Dyson equation in the energy domain [46],

$$G^r(\epsilon) = [1 - G_0^r(\epsilon) \Sigma^r(\epsilon)]^{-1} G_0^r(\epsilon), \quad (12)$$

where $G_0^r(\epsilon)$ is the retarded Green's function of the isolated central region in the energy domain. Combining Eq. (11) with Eq. (12), we have $A(\epsilon, \sigma) = \frac{1}{\sigma} G^r(\epsilon + i\sigma)$. The spectral function can be finally obtained from inverse Laplace transformation by changing the variable $i\sigma \rightarrow \omega - \epsilon + i0^+$,

$$\begin{aligned} A(\epsilon, t) &= \int \frac{d\omega}{2\pi i} \frac{e^{-i(\omega-\epsilon)t}}{\epsilon - \omega - i0^+} G^r(\omega) \\ &= G^r(\epsilon) + \int \frac{d\omega}{2\pi i} \frac{e^{-i(\omega-\epsilon)t}}{\epsilon - \omega + i0^+} G^r(\omega). \end{aligned} \quad (13)$$

Moreover, it is easy to obtain the retarded Green's function $G^r(t_1, t_2)$ from the spectral function,

$$\begin{aligned} G^r(t_1, t_2) &= \int \frac{d\epsilon}{2\pi} A(\epsilon, t_1) e^{-i\epsilon(t_1-t_2)} \\ &= \int \frac{d\omega}{2\pi i} G^r(\omega) e^{-i\omega t_1} \int \frac{d\epsilon}{2\pi} \frac{e^{i\epsilon t_2}}{\epsilon - \omega - i0^+} \\ &= G^r(t_1 - t_2). \end{aligned} \quad (14)$$

Here, we have used the relation $\int \frac{d\epsilon}{2\pi} \frac{e^{i\epsilon t_2}}{\epsilon - \omega - i0^+} = i e^{i\omega t_2}$ ($t_2 > 0$). We would like to emphasize that the retarded Green's function in the transient regime within the Caroli scheme is the same as the one in the steady state which is a function of time difference even beyond the WBL. However, this is only valid for dc transport and transient dynamics under the upward or downward steplike pulse at $t = 0$ because in these cases, no ac bias is present at $t > 0$.

The lesser Green's function $G^<(t_1, t_2)$ satisfies the Keldysh equation [18,28],

$$\begin{aligned} G^<(t_1, t_2) &= G^r(t_1, 0) G^<(0, 0) G^a(0, t_2) \\ &+ \int_0^t dt_3 \int_0^t dt_4 G^r(t_1, t_3) \Sigma^<(t_3, t_4) G^a(t_4, t_2). \end{aligned} \quad (15)$$

Here, $G^<(0, 0)$ is the initial occupation of the central region that may affect the transient electric and energy currents. For simplicity, we assume that the occupation of the central region is empty initially and then the first term on the right side is neglected. This is mainly because the local density of states of the central region is a smooth function in the limit $t_1(t_2) \rightarrow \infty$ [47]. However, if bound states are present in the central region, the contribution of the initial occupation then becomes important to the time-dependent quantum transport.

After substituting Eqs. (5) and (7) into Eq. (15), we have

$$G^<(t_1, t_2) = \int \frac{d\epsilon}{2\pi} A(\epsilon, t_1) \Sigma^<(\epsilon) A^\dagger(\epsilon, t_2) e^{-i\epsilon(t_1-t_2)}. \quad (16)$$

Finally, we can obtain the exact solution for the transient electric and energy currents beyond the WBL within the Caroli scheme (see details in Appendix A),

$$\begin{aligned} I_\alpha^X(t) &= \int \frac{d\epsilon}{2\pi} \text{Tr}[A(\epsilon, t) \Sigma^<(\epsilon) B_\alpha^X(\epsilon, t) \\ &+ A(\epsilon, t) \Sigma_\alpha^{<,X}(\epsilon)] + \text{H.c.}, \end{aligned} \quad (17)$$

where

$$B_\alpha^X(\epsilon, t) = \int \frac{d\omega}{-2\pi i} G^a(\omega) \Sigma_\alpha^{a,X}(\omega) \frac{e^{i(\omega-\epsilon)t}}{\epsilon - \omega + i0^+}. \quad (18)$$

At the end of this subsection, it is worth noting that the exact solution of transient electric and energy currents we obtained within the Caroli scheme is a general solution for the case of a quench in a noninteracting system since the initial state of the two-probe mesoscopic system is described by a time-independent Hamiltonian and the propagation of this system is also governed by another time-independent Hamiltonian.

B. Shot noise of electric and energy current in the transient regime

The current can fluctuate around its average since the quantum transport is stochastic in nature [48]. It is important to study the noise spectra which contain useful information that characterizes quantum transport in mesoscopic systems. Recently, the time-dependent current correlations and thermal noise within the WBL were studied based on the Caroli scheme [49]. The current and heat fluctuations were also extensively investigated from full counting statistics [32,50,51]. In this subsection, the transient shot noise of electric and energy currents within the Caroli scheme will be studied. The fluctuations of electric and energy current can be defined as

$$F_\alpha^\chi(t) \equiv \langle \Delta I_\alpha^\chi(t)^2 \rangle = \langle [I_\alpha^\chi(t)]^2 \rangle - \langle I_\alpha^\chi(t) \rangle^2. \quad (19)$$

By using Eq. (2), we can obtain [52,53]

$$\begin{aligned} F_\alpha^\chi(t) = & - \sum_{\mathbf{k}\mathbf{k}'mn} \epsilon_{\mathbf{k}\alpha}^\chi \epsilon_{\mathbf{k}'\alpha}^\chi [t_{\mathbf{k}\alpha m} t_{\mathbf{k}'\alpha n} (\langle c_{\mathbf{k}\alpha}^\dagger d_m c_{\mathbf{k}'\alpha}^\dagger d_n \rangle \\ & - \langle c_{\mathbf{k}\alpha}^\dagger d_m \rangle \langle c_{\mathbf{k}'\alpha}^\dagger d_n \rangle) + t_{\mathbf{k}\alpha m}^* t_{\mathbf{k}'\alpha n}^* (\langle d_m^\dagger c_{\mathbf{k}\alpha} c_{\mathbf{k}'\alpha}^\dagger d_n^\dagger \rangle \\ & - \langle d_m^\dagger c_{\mathbf{k}\alpha} \rangle \langle d_n^\dagger c_{\mathbf{k}'\alpha} \rangle) - t_{\mathbf{k}\alpha m} t_{\mathbf{k}'\alpha n}^* (\langle c_{\mathbf{k}\alpha}^\dagger d_m d_n^\dagger c_{\mathbf{k}'\alpha} \rangle) \end{aligned}$$

$$\begin{aligned} & - \langle c_{\mathbf{k}\alpha}^\dagger d_m \rangle \langle d_n^\dagger c_{\mathbf{k}'\alpha} \rangle) - t_{\mathbf{k}\alpha m}^* t_{\mathbf{k}'\alpha n} (\langle d_m^\dagger c_{\mathbf{k}\alpha} c_{\mathbf{k}'\alpha}^\dagger d_n \rangle \\ & - \langle d_m^\dagger c_{\mathbf{k}\alpha} \rangle \langle c_{\mathbf{k}'\alpha}^\dagger d_n \rangle)]. \quad (20) \end{aligned}$$

Applying Wick's theorem, Eq. (20) becomes

$$\begin{aligned} F_\alpha^\chi(t) = & - \sum_{\mathbf{k}\mathbf{k}'mn} \epsilon_{\mathbf{k}\alpha}^\chi \epsilon_{\mathbf{k}'\alpha}^\chi [t_{\mathbf{k}\alpha m} t_{\mathbf{k}'\alpha n} \langle c_{\mathbf{k}\alpha}^\dagger d_m \rangle \langle d_m c_{\mathbf{k}'\alpha}^\dagger \rangle \\ & + t_{\mathbf{k}\alpha m}^* t_{\mathbf{k}'\alpha n}^* \langle d_m^\dagger c_{\mathbf{k}\alpha} \rangle \langle c_{\mathbf{k}\alpha} d_n^\dagger \rangle \\ & - t_{\mathbf{k}\alpha m} t_{\mathbf{k}'\alpha n}^* \langle c_{\mathbf{k}\alpha}^\dagger c_{\mathbf{k}'\alpha} \rangle \langle d_m d_n^\dagger \rangle \\ & - t_{\mathbf{k}\alpha m}^* t_{\mathbf{k}'\alpha n} \langle d_m^\dagger d_n \rangle \langle c_{\mathbf{k}\alpha} c_{\mathbf{k}'\alpha}^\dagger \rangle], \quad (21) \end{aligned}$$

which can be written in terms of NEGF [52,53],

$$\begin{aligned} F_\alpha^\chi(t) = & - \sum_{\mathbf{k}\mathbf{k}'mn} \epsilon_{\mathbf{k}\alpha}^\chi \epsilon_{\mathbf{k}'\alpha}^\chi [t_{\mathbf{k}\alpha m} t_{\mathbf{k}'\alpha n} G_{n,\mathbf{k}\alpha}^<(t,t) G_{m,\mathbf{k}'\alpha}^>(t,t) \\ & + t_{\mathbf{k}\alpha m}^* t_{\mathbf{k}'\alpha n}^* G_{\mathbf{k}'\alpha,m}^<(t,t) G_{\mathbf{k}\alpha,n}^>(t,t) \\ & - t_{\mathbf{k}\alpha m} t_{\mathbf{k}'\alpha n}^* G_{\mathbf{k}'\alpha,\mathbf{k}\alpha}^<(t,t) G_{mn}^>(t,t) \\ & - t_{\mathbf{k}\alpha m}^* t_{\mathbf{k}'\alpha n} G_{mn}^<(t,t) G_{\mathbf{k}\alpha,\mathbf{k}'\alpha}^>(t,t)]. \quad (22) \end{aligned}$$

After the analytic continuation, the shot noise of electric and energy current can be expressed as

$$\begin{aligned} F_\alpha^\chi(t) = & \text{Tr} \left\{ -2\text{Re} \left[\left(\int dt_1 G^r(t, t_1) \Sigma_\alpha^{<,\chi}(t_1, t) + G^<(t, t_1) \Sigma_\alpha^{a,\chi}(t_1, t) \right) \left(\int dt_1 G^r(t, t_1) \Sigma_\alpha^{>,\chi}(t_1, t) + G^>(t, t_1) \Sigma_\alpha^{a,\chi}(t_1, t) \right) \right] \right. \\ & + G^>(t, t) \left[\int dt_1 \int dt_2 [2i\text{Im}(\Sigma_\alpha^{r,\chi}(t, t_1) G^r(t_1, t_2) \Sigma_\alpha^{<,\chi}(t_2, t)) + \Sigma_\alpha^{r,\chi}(t, t_1) G^<(t_1, t_2) \Sigma_\alpha^{a,\chi}(t_2, t)] + \Sigma_\alpha^{<,2\chi}(t, t) \right] \\ & \left. + G^<(t, t) \left[\int dt_1 \int dt_2 [2i\text{Im}(\Sigma_\alpha^{r,\chi}(t, t_1) G^r(t_1, t_2) \Sigma_\alpha^{>,\chi}(t_2, t)) + \Sigma_\alpha^{r,\chi}(t, t_1) G^>(t_1, t_2) \Sigma_\alpha^{a,\chi}(t_2, t)] + \Sigma_\alpha^{>,2\chi}(t, t) \right] \right\}. \quad (23) \end{aligned}$$

For the time-dependent transport behavior within the Caroli scheme, the shot noise can be expressed using the spectral function $A(\epsilon, t)$ (see details in Appendix B),

$$\begin{aligned} F_\alpha^\chi(t) = & \text{Tr} \int \frac{d\epsilon}{2\pi} [-2\text{Re}[F_{\alpha,1}^<(\epsilon, t) F_{\alpha,1}^>(\epsilon, t)] + G^<(\epsilon, t) [2i\text{Im}[F_{\alpha,2}^<(\epsilon, t)] + F_{\alpha,3}^<(\epsilon, t) + \Sigma_\alpha^{<,2\chi}(\epsilon)] \\ & + G^>(\epsilon, t) [2i\text{Im}[F_{\alpha,2}^>(\epsilon, t)] + F_{\alpha,3}^>(\epsilon, t) + \Sigma_\alpha^{>,2\chi}(\epsilon)]]. \quad (24) \end{aligned}$$

Here,

$$G^{<(>)}(\epsilon, t) = A(\epsilon, t) \Sigma^{<(>)}(\epsilon) A^\dagger(\epsilon, t), \quad (25)$$

$$F_{\alpha,1}^{<(>)}(\epsilon, t) = A_\alpha(\epsilon, t) \Sigma_\alpha^{<(>,\chi)}(\epsilon) + A(\epsilon, t) \Sigma^{<(>)}(\epsilon) B_\alpha^\chi(\epsilon, t), \quad (26)$$

$$F_{\alpha,2}^{<(>)}(\epsilon, t) = \int \frac{d\epsilon_1}{2\pi} \frac{ie^{-i(\epsilon-\epsilon_1)t}}{\epsilon - \epsilon_1 + i0^+} \Sigma_\alpha^{r,\chi}(\epsilon) G^r(\epsilon) \Sigma_\alpha^{<(>,\chi)}(\epsilon_1), \quad (27)$$

$$F_{\alpha,3}^{<(>)}(\epsilon, t) = \int \frac{d\epsilon_1}{2\pi} \int \frac{d\omega}{2\pi} \frac{e^{-i(\epsilon-\epsilon_1)t}}{(\epsilon - \omega + i0^+)(\epsilon_1 - \omega - i0^+)} \Sigma_\alpha^{r,\chi}(\epsilon) G^r(\epsilon) \Sigma^{<(>)}(\omega) G^a(\epsilon_1) \Sigma_\alpha^{a,\chi}(\epsilon_1). \quad (28)$$

C. Thermoelectric effect

In this subsection, the time-dependent thermoelectric effect in the transient regime within the Caroli scheme will be investigated. We assume that the applied biases of the left and right lead are $V_L = \Delta V$ and $V_R = 0$, respectively. In order to study the thermoelectric effect, a temperature gradient between two leads is introduced by setting the temperatures of the left

and right lead to be $T_L = T_0 + \Delta T$ and $T_R = T_0$, respectively. It can be found in Eq. (17) that $A(\epsilon, t)$ and $B_\alpha^\chi(\epsilon, t)$ only depend on the applied bias while $\Sigma_L^{<,\chi}(\epsilon)$ depends on both the applied bias ΔV and the temperature gradient ΔT . In the linear response regime, namely, under small bias voltage and small temperature gradient, the retarded Green's function in the steady state $G^r(\epsilon)$ can be expanded to the first order in

ΔV according to the Dyson equation [54,55],

$$G^r(\epsilon) = \tilde{G}^r(\epsilon) - \tilde{G}^r(\epsilon) \frac{\partial \tilde{\Sigma}_L^r(\epsilon)}{\partial \epsilon} \tilde{G}^r(\epsilon) \Delta V. \quad (29)$$

Here, the superscript ' \sim ' is used to denote the quantities in the absence of applied bias and temperature gradient. Similarly, the Fermi-Dirac distribution can be expanded as ($k_B = 1$ for simplicity)

$$f_L(\epsilon + \Delta V) = \tilde{f}(\epsilon) + \frac{\partial \tilde{f}}{\partial \epsilon} \Delta V - \frac{\epsilon}{T} \frac{\partial \tilde{f}}{\partial \epsilon} \Delta T, \quad (30)$$

where $\tilde{f}(\epsilon)$ is the Fermi function of leads at temperature T_0 and zero applied bias. Therefore, the transient electric current in the left lead can be expressed as

$$I_L^0(t) = \tilde{I}_L^0(t) + G_V^0(t) \Delta V + G_T^0(t) \Delta T. \quad (31)$$

Here, $\tilde{I}_L^0(t)$ is the equilibrium transient electric current of the left lead in the absence of voltage gradient and temperature gradient. It is solely contributed from the switching of the coupling between the quantum dot and leads and can be given by

$$\begin{aligned} \tilde{I}_L^0(t) = & \int \frac{d\epsilon}{2\pi} \text{Tr}[\tilde{A}(\epsilon, t) \tilde{\Sigma}^<(\epsilon) \tilde{B}_L^0(\epsilon, t) \\ & + \tilde{A}(\epsilon, t) \tilde{\Sigma}_L^<,0(\epsilon)] + \text{H.c.} \end{aligned} \quad (32)$$

$G_V^0(t)$ is the electric conductance of the left lead [56],

$$\begin{aligned} G_V^0(t) = & \int \frac{d\epsilon}{2\pi} \text{Tr}[A_V(\epsilon, t) \tilde{\Sigma}^<(\epsilon) \tilde{B}_L^0(\epsilon, t) \\ & + \tilde{A}(\epsilon, t) \Sigma_V^<,0(\epsilon) \tilde{B}_L^0(\epsilon, t) + \tilde{A}(\epsilon, t) \tilde{\Sigma}^<(\epsilon) B_V^0(\epsilon, t) \\ & + A_V(\epsilon, t) \tilde{\Sigma}_L^<,0(\epsilon) + \tilde{A}(\epsilon, t) \Sigma_V^<,0(\epsilon)] + \text{H.c.}, \end{aligned} \quad (33)$$

and $G_{T,L}^0(t)$ is the thermal coefficient of the left lead,

$$\begin{aligned} G_T^0(t) = & \int \frac{d\epsilon}{2\pi} \text{Tr}[\tilde{A}(\epsilon, t) \Sigma_T^<,0(\epsilon) \tilde{B}_L^0(\epsilon, t) \\ & + \tilde{A}(\epsilon, t) \Sigma_T^<,0(\epsilon)] + \text{H.c.} \end{aligned} \quad (34)$$

Here, we have

$$A_V(\epsilon, t) = \int \frac{d\omega}{2\pi i} \left[\tilde{G}^r(\omega) \frac{\partial \tilde{\Sigma}_L^{r,0}(\omega)}{\partial \omega} \tilde{G}^r(\omega) \right] \frac{e^{-i(\omega-\epsilon)t}}{\epsilon - \omega - i0^+}, \quad (35)$$

$$\begin{aligned} B_V^0(\epsilon, t) = & \int \frac{d\omega}{-2\pi i} \left[\tilde{G}^a(\omega) \frac{\partial \tilde{\Sigma}_L^{a,0}(\omega)}{\partial \omega} \tilde{G}^a(\omega) \tilde{\Sigma}_L^{a,0}(\omega) \right. \\ & \left. + \tilde{G}^a(\omega) \frac{\partial \tilde{\Sigma}_L^{a,0}(\omega)}{\partial \omega} \right] \frac{e^{i(\omega-\epsilon)t}}{\epsilon - \omega + i0^+}, \end{aligned} \quad (36)$$

$$\Sigma_V^<,0(\epsilon) = \frac{\partial \tilde{\Sigma}_L^<,0(\epsilon)}{\partial \epsilon}, \quad (37)$$

$$\Sigma_T^<,0(\epsilon) = i\tilde{\Gamma}_L(\epsilon) \frac{\epsilon}{T_0} \frac{\partial \tilde{f}(\epsilon)}{\partial \epsilon}, \quad (38)$$

where $\tilde{\Gamma}_L(\epsilon)$ is the linewidth function of left lead with $\Delta V = 0$.

In order to obtain the time-dependent thermoelectric coefficient, we can rewrite Eq. (31) as

$$\Delta I_L^0(t) = I_L^0(t) - \tilde{I}_L^0(t) = G_V^0(t) \Delta V + G_T^0(t) \Delta T. \quad (39)$$

By setting $\Delta I_L^0(t) = 0$, namely, the transient electric current induced by the external bias ΔV and that induced by the temperature gradient ΔT have canceled out each other, the time-dependent Seebeck coefficient in the transient regime can be obtained,

$$S_L^0(t) = -\frac{\Delta V}{\Delta T} = \frac{G_T^0(t)}{G_V^0(t)}. \quad (40)$$

D. Single-level model within WBL

In the above, we have obtained the exact solutions of the time-dependent electric and energy currents, shot noise, and thermoelectric coefficient in the transient regime which are quite general and goes beyond the WBL. In this subsection, we will apply these solutions to the simplest model, namely, a single-level quantum dot within the WBL. In this model, the second term of Hamiltonian in Eq. (1) that describes the quantum dot is given by $\epsilon_0 d^\dagger d$ and the self-energy can be simply given by $\Sigma_\alpha^{r,a,\chi}(\epsilon) = \mp i\epsilon^\chi \Gamma_\alpha / 2$ and $\Sigma_\alpha^{<, >, \chi}(\epsilon) = i\epsilon^\chi f_\alpha(\epsilon) \Gamma_\alpha$ where Γ_α is the linewidth amplitude. The retarded Green's function in the steady state can be expressed as

$$G^r(\epsilon) = \frac{1}{\epsilon - \epsilon_0 + \frac{i}{2}\Gamma}, \quad (41)$$

where $\Gamma = \sum_\alpha \Gamma_\alpha$ is the total linewidth amplitude. Then the spectral function $A(\epsilon, t)$ defined in Eq. (13) can be given by

$$A(\epsilon, t) = G^r(\epsilon) [1 - e^{i(\epsilon - \epsilon_0 + \frac{i}{2}\Gamma)t}], \quad (42)$$

and $B_\alpha^\chi(\epsilon, t)$ can be given as

$$B_\alpha^\chi(\epsilon, t) = G^a(\epsilon) \Sigma_\alpha^{a,0}(\epsilon) \left[\epsilon^\chi - \left(\epsilon_0 + \frac{i}{2}\Gamma \right)^\chi e^{-i(\epsilon - \epsilon_0 - \frac{i}{2}\Gamma)t} \right]. \quad (43)$$

The transient electric and energy currents and their fluctuations within the WBL can be obtained from Eqs. (17) and (24).

Similarly, the time-dependent Seebeck coefficient within the WBL can be obtained from Eq. (40),

$$S_L^0(t) = \frac{\int d\epsilon \frac{\partial \tilde{f}(\epsilon)}{\partial \epsilon} \epsilon \mathcal{T}(\epsilon, t)}{T_0 \int d\epsilon \frac{\partial \tilde{f}(\epsilon)}{\partial \epsilon} \mathcal{T}(\epsilon, t)}, \quad (44)$$

where $\mathcal{T}(\epsilon, t)$ is the time-dependent transmission coefficient,

$$\mathcal{T}(\epsilon, t) = -A(\epsilon, t) \Gamma_L A^\dagger(\epsilon, t) \Gamma_L - 2\text{Im}[A(\epsilon, t)] \Gamma_L. \quad (45)$$

This expression of transient Seebeck coefficient within the WBL is similar to that reported within the Cini scheme [30].

In the short-time limit, namely, for small t , the time-dependent electric and energy current within the Caroli scheme can be given by

$$I_\alpha^\chi(t) = 2\Gamma_\alpha t \int \frac{d\epsilon}{2\pi} \epsilon^\chi f_\alpha(\epsilon). \quad (46)$$

It is found that at short times, the slopes of both transient electric and energy currents are independent of the energy level of quantum dot. The transient Seebeck coefficient in the

short-time limit can be expressed as

$$S_L^0(t) = \frac{\epsilon_0 \int \frac{d\epsilon}{2\pi} \frac{\partial \tilde{f}(\epsilon)}{\partial \epsilon} \epsilon^2}{3T_0 \int \frac{d\epsilon}{2\pi} \frac{\partial \tilde{f}(\epsilon)}{\partial \epsilon}} t^2. \quad (47)$$

In contrast to the transient electric and energy current, the transient Seebeck coefficient at short times is of order t^2 . The first-order transient Seebeck coefficients of t is zero since $\frac{\partial \tilde{f}(\epsilon)}{\partial \epsilon}$ is an even function of energy when the Fermi energy is set to zero.

E. Single-level model with Lorentzian linewidth

In this subsection, we will apply the exact solutions to a single-level quantum dot with Lorentzian linewidth to model the finite bandwidth effects. The Lorentzian linewidth function is defined as

$$\Gamma_\alpha(\epsilon) = \frac{\Gamma_\alpha W^2}{(\epsilon - V_\alpha)^2 + W^2}, \quad (48)$$

where Γ_α is the linewidth amplitude and W is the bandwidth. Then the self-energy can be expressed as [16]

$$\Sigma_\alpha^{r,a,\chi}(\epsilon) = \int \frac{d\omega}{2\pi} \frac{\epsilon^\chi \Gamma_\alpha(\omega)}{\epsilon - \omega \pm i0^+} = \frac{1}{2} \frac{\epsilon^\chi \Gamma_\alpha W}{\epsilon - V_\alpha \pm iW}. \quad (49)$$

The retarded Green's function in the steady state can be expressed as

$$G^r(\epsilon) = \frac{1}{\epsilon - \epsilon_0 - \frac{1}{2} \sum_\alpha \frac{\Gamma_\alpha W}{\epsilon - V_\alpha + iW}}. \quad (50)$$

To simplify the algebra, we assume that $V_R = 0$ and $V_L \neq 0$ without loss of generality. The retarded Green's function in the steady state can then be written as [16]

$$G^r(\epsilon) = \frac{(\epsilon - V_L + iW)(\epsilon + iW)}{(\epsilon - \omega_1)(\epsilon - \omega_2)(\epsilon - \omega_3)}, \quad (51)$$

where ω_1, ω_2 , and ω_3 are the poles of $G^r(\epsilon)$ (see details in Appendix C). The spectral function $A(\epsilon, t)$ can be rewritten as

$$A(\epsilon, t) = G^r(\epsilon) + \sum_{i=1}^3 \frac{(\omega_i - V_L + iW)(\omega_i + iW)}{\prod_{j \neq i} (\omega_i - \omega_j)} \frac{e^{-i(\omega_i - \epsilon)t}}{(\omega_i - \epsilon)}, \quad (52)$$

and $B_\alpha^X(\epsilon, t)$ can be expressed as

$$B_\alpha^X(\epsilon, t) = G^a(\epsilon) \Sigma_\alpha^{a,\chi}(\epsilon) + \sum_{i=1}^3 \frac{(\omega_i^* - V_L - iW)(\omega_i^* - iW)}{\prod_{j \neq i} (\omega_i^* - \omega_j^*)} \times \frac{1}{2} \frac{e^{i(\omega_i^* - \epsilon)t} \Gamma_\alpha W (\omega_i^*)^\chi}{(\omega_i^* - \epsilon)(\omega_i^* - V_\alpha - iW)}. \quad (53)$$

By applying Eqs. (52) and (53), the time-dependent electric and energy currents in the transient regime for a single-level quantum dot system can be numerically calculated from Eq. (17) and the corresponding transient shot noise can be calculated from Eq. (24).

Similarly, the time-dependent thermoelectric coefficient in the transient regime of a single-level model can be investigated. In the absence of applied bias and temperature gradient, the retarded Green's function $\tilde{G}^r(\epsilon)$ can be rewritten as

$$\tilde{G}^r(\epsilon) = \frac{\epsilon + iW}{(\epsilon - \tilde{\omega}_1)(\epsilon - \tilde{\omega}_2)}, \quad (54)$$

with

$$\tilde{\omega}_{1,2} = \frac{\epsilon_0 - iW \pm \sqrt{(\epsilon_0 + iW)^2 + 2\Gamma W}}{2}. \quad (55)$$

With the poles of the Green's functions explicitly known, the thermoelectric coefficients $G_{V,\alpha}^X(t)$ and $G_{T,\alpha}^X(t)$ defined in Eqs. (33) and (34) can be calculated using the residue theorem (see details in Appendix D), respectively. The time-dependent Seebeck coefficient of a single-level quantum dot can then be obtained from Eq. (40).

III. NUMERICAL RESULTS

The time-dependent electric and energy currents of a single-level quantum dot model with Lorentzian linewidth induced by the temperature gradient are calculated numerically. The temperatures of left and right leads are set to be $T_L = 0.5\Gamma$ and $T_R = 0$, respectively. The external biases of both leads are set to be zero. We assume that the linewidth amplitude is $\Gamma_L = \Gamma_R = 0.5\Gamma$ and the bandwidth W is same for both leads.

The transient electric and energy currents for different energy levels of the quantum dot ϵ_0 with the bandwidth $W = 5\Gamma$ is plotted in Fig. 1. Once the coupling between the leads and quantum dot is turned on, the transient electric and energy currents increase first and then approach to the dc steady state that can be calculated from the Landauer-Büttiker formula in the long-time limit. It is found that both the electric and energy currents in the steady state decrease with the increasing energy levels. The oscillation frequency of both transient electric and energy currents is proportional to the energy level of the quantum dot. The oscillation behavior can be simply explained within the WBL. The oscillation of transient electric and energy currents is induced by the oscillation term $e^{i(\epsilon - \epsilon_0 + \frac{1}{2}\Gamma)t}$ in the spectral function $A(\epsilon, t)$ in Eq. (42) within the WBL. Therefore, the period of oscillation is proportional to the energy level ϵ_0 of the quantum dot. In addition, the damping of the oscillation is dominated by the lifetime of the resonant state of the quantum dot which is proportional to the linewidth amplitude Γ in the WBL.

Figure 2 presents the transient electric and energy currents with different bandwidths. The energy level of the quantum dot is chosen to be $\epsilon_0 = 1\Gamma$. The time-dependent electric and energy currents in the transient regime exhibit similar behavior under temperature gradients. Both the electric and energy currents in the steady state increase with the increasing bandwidth W since the energy broadening of the quantum dot becomes smaller. When the bandwidth is large, the time-dependent electric and energy currents converge to results within the WBL. Moreover, the oscillation of transient electric and energy currents becomes more significant as the bandwidth decreases which means that more relaxation time is needed for the system to reach the steady state. We note that

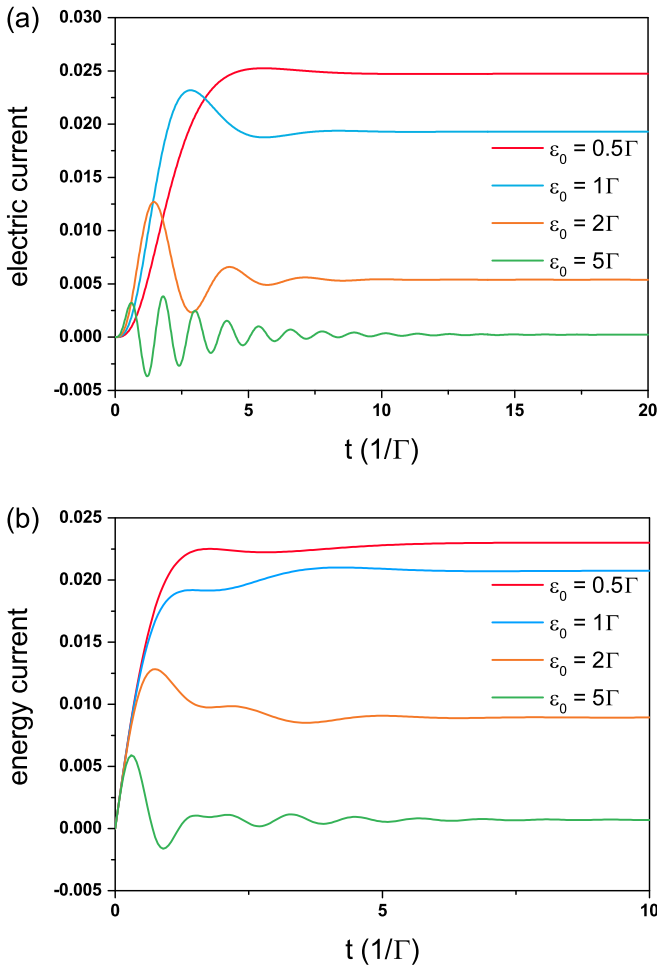


FIG. 1. (a) Transient electric current and (b) transient energy current with different energy levels of quantum dot ϵ_0 . The bandwidth is set to be $W = 5\Gamma$ and the temperatures of left and right leads are set to be $T_L = 0.5\Gamma$ and $T_R = 0$, respectively.

the damping of oscillations is dominated by the linewidth amplitude Γ in the WBL. In the Lorentzian model, the linewidth function is determined by the bandwidth W in Eq. (48). Therefore, the lifetime of resonant states is proportional to the bandwidth resulting in the faster decay rate of transient electric and energy currents for the system with a larger bandwidth.

The time-dependent shot noise of electric and energy currents induced by the temperature gradient with different bandwidths is then investigated. The energy level of the quantum dot is chosen to be $\epsilon_0 = 1\Gamma$. The external biases of both leads are set to be zero and the temperatures of left and right leads are set to be $T_L = 0.1\Gamma$ and $T_R = 0$, respectively. In Fig. 3, both $F_L^0(t)$ and $F_L^1(t)$ increase abruptly to a maximum value and then gradually approach to the fluctuations at equilibrium. The larger steady-state fluctuations for both electric and energy currents are found in the system with a larger bandwidth W which gives rise to a higher number of electrons incoming from the leads and traversing the scattering region. The oscillation of transient fluctuations $F_L^0(t)$ and $F_L^1(t)$ becomes more notable as the bandwidth decreases, which agrees with

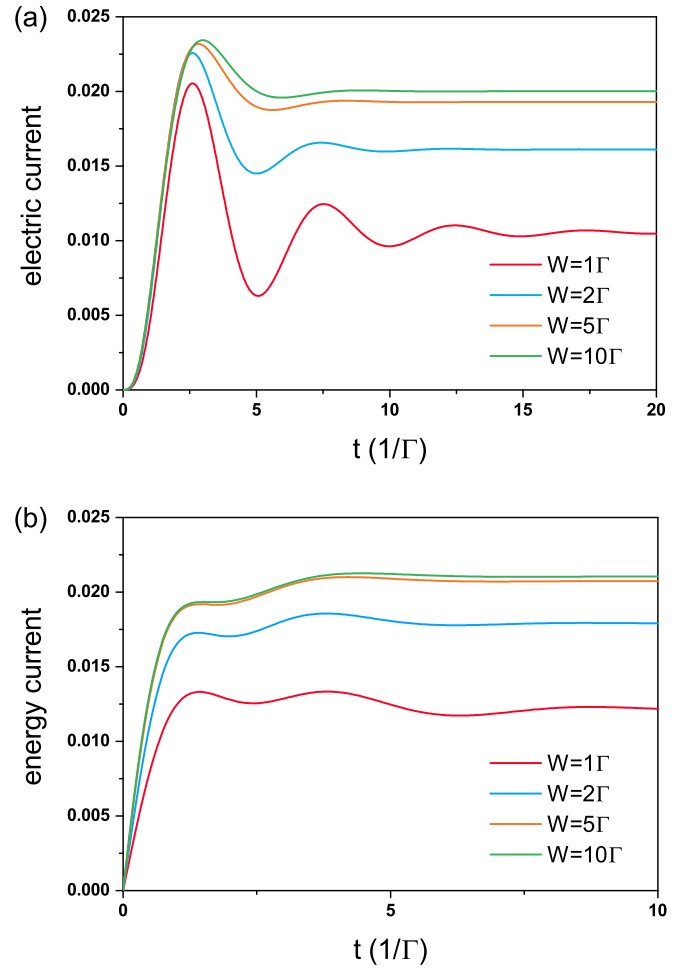


FIG. 2. (a) Transient electric current and (b) transient energy current with different bandwidths W of leads. The energy level of the quantum dot is set to be $\epsilon_0 = 1\Gamma$ and the temperatures of left and right leads are set to be $T_L = 0.5\Gamma$ and $T_R = 0$, respectively.

that of the transient electric and energy currents as presented in Fig. 2.

We now study the time-dependent Seebeck coefficient in the transient regime of a single-level quantum dot with Lorentzian linewidth. The external biases of both leads are still set to be zero and the bandwidths of both leads are assumed to be $W = 10\Gamma$. Figure 4 presents the transient Seebeck coefficient with different energy levels of the quantum dot under a reference temperature of $T_0 = 0.1\Gamma$. It is found that the time-dependent Seebeck coefficient is significantly enhanced in the transient regime. It first raises to reach a maximum value and then approaches the long-time limit. The enhancement of Seebeck coefficient in the transient regime grows with the increasing energy level of the quantum dot. We also find that the time-dependent Seebeck coefficient at short times exhibits quadratic behaviors and increases with the increasing energy level of quantum dot, as shown in the inset of Fig. 4. This agrees well with the expression of the transient Seebeck coefficient within the WBL in the short time limit in Eq. (47). Similar to the transient electric and energy currents, the period of oscillation in the transient Seebeck coefficient is proportional to the energy level of quantum dot.

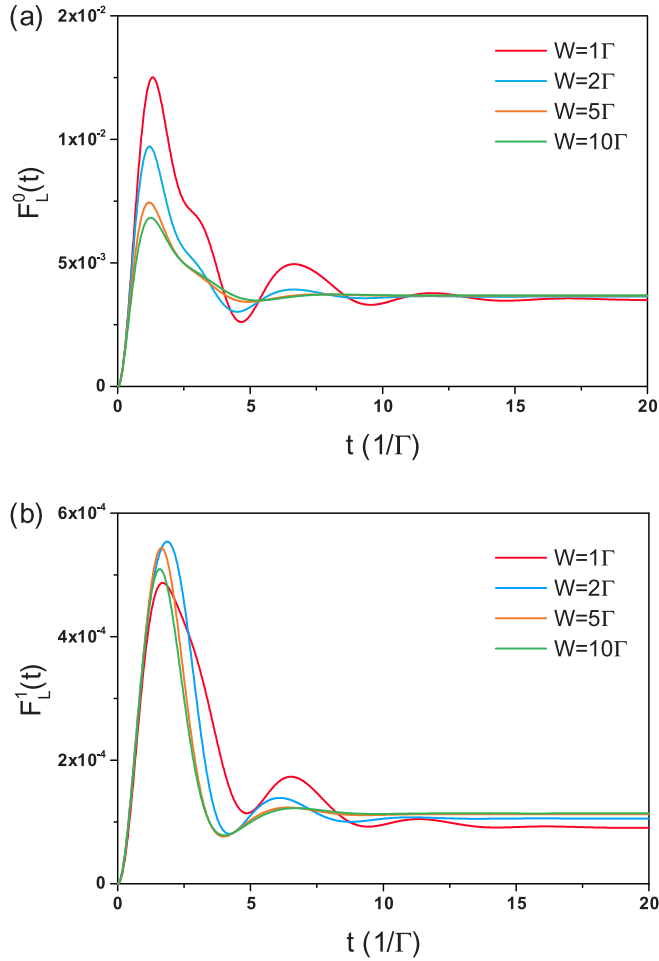


FIG. 3. Time-dependent shot noise of (a) electric and (b) energy currents in the transient regime with different bandwidths W of leads. The energy level of the quantum dot is set to be $\epsilon_0 = 1\Gamma$ and the temperatures of left and right leads are set to be $T_L = 0.1\Gamma$ and $T_R = 0$, respectively.

Moreover, the Seebeck coefficient in the steady state increases with the increasing energy levels of quantum dot first and it then reduces with the increasing energy levels when ϵ_0 exceeds 0.8Γ . From the expression of the transient Seebeck coefficient within the WBL, it can confirm that the integrals in Eq. (44) are mainly contributed by the energy near the Fermi level due to the energy derivative of the Fermi distribution function. When the energy level of quantum dot increases, the corresponding transmission peak goes away from the Fermi level. Therefore, the Seebeck coefficient in the long-time limit is enhanced due to the increasing energy levels of the quantum dot when the energy levels are small.

The transient Seebeck coefficients under different reference temperatures T_0 with the energy level $\epsilon_0 = 0.5\Gamma$ are plotted in Fig. 5. It is found that the enhancement of transient Seebeck coefficients is significantly improved by the increasing reference temperature in the linear response regime. The elapsed time at which the sharp peaks of transient Seebeck effect occurs and the relaxation time the system needed to reach the steady state are independent of the reference temperature. We also find that the Seebeck coefficient both in the transient regime and in the long-time limit is proportional to

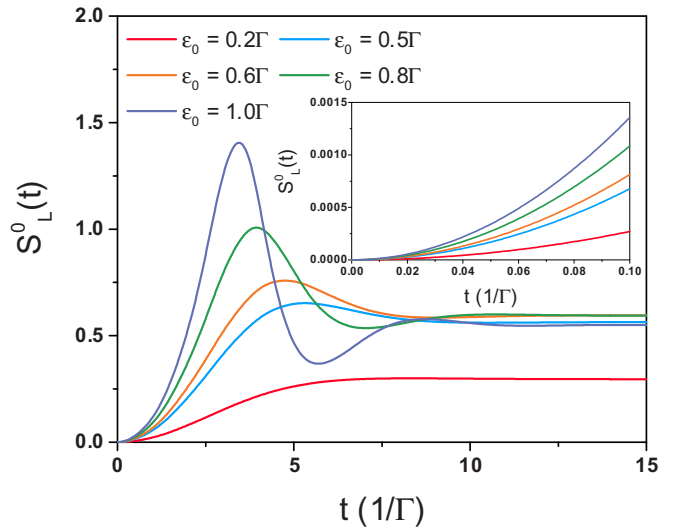


FIG. 4. Time-dependent Seebeck coefficient in the transient regime with different energy levels of quantum dot ϵ_0 . The bandwidth is set to be $W = 10\Gamma$ and the reference temperature of leads is set to be $T_0 = 0.1\Gamma$. (Inset) Transient Seebeck coefficient at short times.

the reference temperature when the reference temperature is small.

IV. CONCLUSION

In summary, the exact solution of time-dependent electric and energy currents, as well as their fluctuations under a quantum quench were obtained within the Caroli scheme. Our theory is based on the NEGF theory and goes beyond the WBL. The transient thermopower in the linear response regime was also obtained. The formalism was then applied to study the transient behavior of a single-level quantum dot with Lorentzian linewidth. Intrinsic oscillatory behavior is

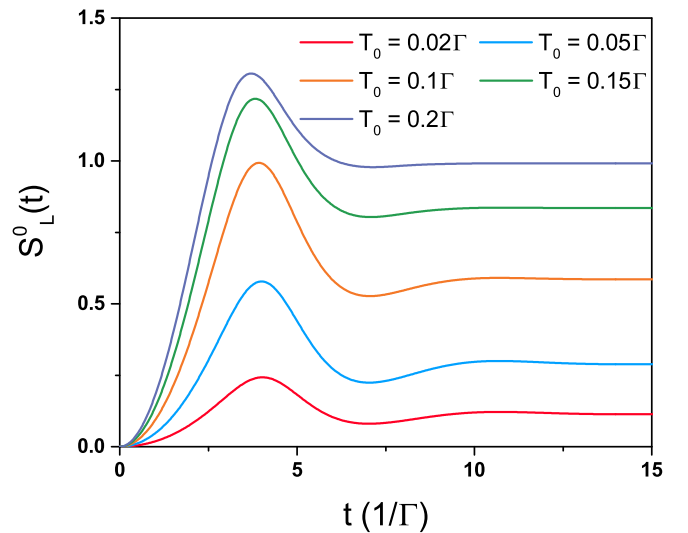


FIG. 5. Time-dependent Seebeck coefficient in the transient regime with different reference temperatures T_0 of leads. The bandwidth is set to be $W = 10\Gamma$ and the energy level of quantum dot is set to be $\epsilon_0 = 0.5\Gamma$.

found in both transient electric and energy currents induced by the temperature gradient. It is found that the oscillatory frequency is proportional to the energy level of quantum dot and the oscillation decays faster for the system with a larger bandwidth. The transient shot noise of electric and energy current also exhibits similar oscillatory behavior. Moreover, significant enhancement of thermopower is observed in the transient regime. The maximum value of the time-dependent Seebeck coefficient increases with both the increasing energy level of quantum dot and the increasing reference temperature of leads.

ACKNOWLEDGMENTS

This work was financially supported by the National Natural Science Foundation of China (Grant No. 11704190), the Jiangsu Provincial Natural Science Foundation of China (Grant No. BK20171030), and the Research Grant Council (Grant No. HKU 17303418).

APPENDIX A: DERIVATION OF TRANSIENT ELECTRIC AND ENERGY CURRENTS

By substituting the expression of $\Sigma_\alpha^{r,\chi}(t_1, t_2)$ in Eq. (5) into Eq. (3), the transient electric and energy currents can be given as

$$I_\alpha^\chi(t) = \int_0^t dt_1 \int \frac{d\epsilon}{2\pi} \text{Tr} \left\{ e^{i\epsilon(t-t_1)} [G^r(t, t_1) \Sigma_\alpha^{<, \chi}(\epsilon) + G^<(t, t_1) \Sigma_\alpha^{a, \chi}(\epsilon)] \right\} + \text{H.c.} \quad (\text{A1})$$

After introducing the spectral function $A(\epsilon, t)$ defined in Eq. (7), the first term in Eq. (A1) can be expressed as

$$\begin{aligned} & \int_0^t dt_1 \int \frac{d\epsilon}{2\pi} \text{Tr} [e^{i\epsilon(t-t_1)} G^r(t, t_1) \Sigma_\alpha^{<, \chi}(\epsilon)] \\ &= \int \frac{d\epsilon}{2\pi} \text{Tr} [A(\epsilon, t) \Sigma_\alpha^{<, \chi}(\epsilon)]. \end{aligned} \quad (\text{A2})$$

Similarly, the second term in Eq. (A1) can be expressed using the spectral function with the help of Eq. (16),

$$\begin{aligned} & \int_0^t dt_1 \int \frac{d\epsilon}{2\pi} \text{Tr} [e^{i\epsilon(t-t_1)} G^<(t, t_1) \Sigma_\alpha^{a, \chi}(\epsilon)] \\ &= \int \frac{d\epsilon}{2\pi} \text{Tr} \left[\int \frac{d\omega}{2\pi} e^{i(\epsilon-\omega)t} A(\omega, t) \Sigma^<(\omega) \right. \\ & \quad \left. \times \int_0^t dt_1 e^{-i(\epsilon-\omega)t_1} A^\dagger(\omega, t_1) \Sigma_\alpha^{a, \chi}(\epsilon) \right]. \end{aligned} \quad (\text{A3})$$

Carrying out directly the integral over t_1 in the above equation, we obtain

$$\begin{aligned} & \int_0^t dt_1 e^{-i(\epsilon-\omega)t_1} A^\dagger(\omega, t_1) \\ &= \int_0^t dt_1 e^{-i(\epsilon-\omega')t_1} \int \frac{d\omega'}{-2\pi i} \frac{1}{\omega - \omega' + i0^+} G^a(\omega') \\ &= \int \frac{d\omega'}{-2\pi i} \frac{i}{\omega' - \epsilon + i0^+} \frac{1}{\omega - \omega' + i0^+} G^a(\omega') \\ &= \frac{i}{\omega - \epsilon + i0^+} G^a(\epsilon). \end{aligned} \quad (\text{A4})$$

Therefore, the second term in Eq. (A1) can be rewritten as

$$\begin{aligned} & \int_0^t dt_1 \int \frac{d\epsilon}{2\pi} \text{Tr} [e^{i\epsilon(t-t_1)} G^<(t, t_1) \Sigma_\alpha^{a, \chi}(\epsilon)] \\ &= \int \frac{d\omega}{2\pi} \text{Tr} [A(\omega, t) \Sigma^<(\omega) B_\alpha^\chi(\omega, t)], \end{aligned} \quad (\text{A5})$$

where

$$B_\alpha^\chi(\omega, t) = \int \frac{d\epsilon}{-2\pi i} \frac{e^{i(\epsilon-\omega)t}}{\omega - \epsilon + i0^+} G^a(\epsilon) \Sigma_\alpha^{a, \chi}(\epsilon). \quad (\text{A6})$$

Then the final expression of transient electric and energy currents in Eq. (17) can be obtained by combining Eqs. (A2) and (A5).

APPENDIX B: EXPRESSION OF TRANSIENT SHOT NOISE USING THE SPECTRAL FUNCTION

In this Appendix, we present the detailed derivation of the final expression for the transient shot noise of electric and energy current. The terms of time-dependent shot noise in Eq. (24) can be rewritten using the spectral function $A_\alpha(\epsilon, t)$.

$$\int dt_1 G^r(t, t_1) \Sigma_\alpha^{<(>), \chi}(t_1, t) = \int \frac{d\epsilon}{2\pi} A_\alpha(\epsilon, t) \Sigma_\alpha^{<(>), \chi}(\epsilon), \quad (\text{B1})$$

$$\begin{aligned} & \int dt_1 G^{<(>)}(t, t_1) \Sigma_\alpha^{a, \chi}(t_1, t) \\ &= \int \frac{d\epsilon}{2\pi} A(\epsilon, t) \Sigma^{<(>)}(\epsilon) B_\alpha^\chi(\epsilon, t), \end{aligned} \quad (\text{B2})$$

$$\begin{aligned} \int dt_1 \int dt_2 \Sigma_\alpha^{r, \chi}(t, t_1) G^r(t_1, t_2) \Sigma_\alpha^{<(>), \chi}(t_2, t) &= \int \frac{d\epsilon}{2\pi} \int \frac{d\epsilon_1}{2\pi} e^{-i(\epsilon-\epsilon_1)t} \Sigma_\alpha^{r, \chi}(\epsilon) \int dt_1 e^{i(\epsilon-\epsilon_1)t_1} A(\epsilon_1, t_1) \Sigma_\alpha^{<(>), \chi}(\epsilon_1) \\ &= \int \frac{d\epsilon}{2\pi} \int \frac{d\epsilon_1}{2\pi} \frac{ie^{-i(\epsilon-\epsilon_1)t}}{\epsilon - \epsilon_1 + i0^+} \Sigma_\alpha^{r, \chi}(\epsilon) G^r(\epsilon) \Sigma_\alpha^{<(>), \chi}(\epsilon_1), \end{aligned} \quad (\text{B3})$$

$$\begin{aligned} & \int dt_1 \int dt_2 \Sigma_\alpha^{r, \chi}(t, t_1) G^{<(>)}(t_1, t_2) \Sigma_\alpha^{a, \chi}(t_2, t) \\ &= \int dt_1 \int dt_2 \int \frac{d\epsilon}{2\pi} e^{-i\epsilon(t-t_1)} \Sigma_\alpha^{r, \chi}(\epsilon) \int \frac{d\omega}{2\pi} A(\omega, t_1) \Sigma^{<(>)}(\omega) A^\dagger(\omega, t_2) e^{-i\omega(t_1-t_2)} \int \frac{d\epsilon_1}{2\pi} e^{i\epsilon_1(t-t_2)} \Sigma_\alpha^{a, \chi}(\epsilon_1) \end{aligned}$$

$$\begin{aligned}
&= \int \frac{d\epsilon}{2\pi} \int \frac{d\epsilon_1}{2\pi} \int \frac{d\omega}{2\pi} e^{-i(\epsilon-\epsilon_1)t} \Sigma_{\alpha}^{\chi,r}(\epsilon) \int dt_1 e^{-i(\omega-\epsilon)t_1} A(\omega, t_1) \Sigma^{<(>)}(\omega) \int dt_2 e^{-i(\epsilon_1-\omega)t_2} A^{\dagger}(\omega, t_2) \Sigma_{\alpha}^{\chi,a}(\epsilon_1) \\
&= \int \frac{d\epsilon}{2\pi} \int \frac{d\epsilon_1}{2\pi} \int \frac{d\omega}{2\pi} \frac{e^{-i(\epsilon-\epsilon_1)t}}{(\epsilon-\omega+i0^+)(\epsilon_1-\omega-i0^+)} \Sigma_{\alpha}^{\chi,r}(\epsilon) G^r(\epsilon) \Sigma^{<(>)}(\omega) G^a(\epsilon_1) \Sigma_{\alpha}^{\chi,a}(\epsilon_1). \tag{B4}
\end{aligned}$$

APPENDIX C: POLES OF $G^r(\epsilon)$

For the single-level quantum dot model with Lorentzian linewidth, the poles of $G^r(\epsilon)$ can be obtained from Eq. (51) [16],

$$\omega_1 = -\frac{b}{3} + \left(\frac{2}{Q}\right)^{\frac{1}{3}} \left(c + \frac{b^2}{3}\right) + \frac{1}{3} \left(\frac{Q}{2}\right)^{\frac{1}{3}}, \tag{C1}$$

$$\omega_2 = -\frac{b}{3} - \frac{1+i\sqrt{3}}{2^{2/3}Q^{1/3}} \left(c + \frac{b^2}{3}\right) - \frac{1-i\sqrt{3}}{6} \left(\frac{Q}{2}\right)^{\frac{1}{3}}, \tag{C2}$$

and

$$\omega_3 = -\frac{b}{3} - \frac{1-i\sqrt{3}}{2^{2/3}Q^{1/3}} \left(c + \frac{b^2}{3}\right) - \frac{1+i\sqrt{3}}{6} \left(\frac{Q}{2}\right)^{\frac{1}{3}}, \tag{C3}$$

with

$$b = 2iW - \epsilon_0 - V_L, \tag{C4}$$

$$c = \frac{\Gamma W}{2} + (W + iV_L)W + \epsilon_0(2iW - V_L), \tag{C5}$$

$$d = \epsilon_0(W + iV_L)W + \frac{W}{2}(\Gamma_R V_L - i\Gamma W), \tag{C6}$$

$$Q = -2b^3 - 9bc - 27d + \theta, \tag{C7}$$

$$\theta = \sqrt{(2b^3 + 9bc + 27d)^2 - 4(b^2 + 3c)^3}. \tag{C8}$$

APPENDIX D: CALCULATION OF THERMOELECTRIC COEFFICIENT $G_{V,L}^0(t)$ AND $G_{T,L}^0(t)$

With the poles of the Green's functions and Lorentzian linewidth function, all quantities in the thermoelectric coefficients $G_{V,\alpha}^{\chi}(t)$ and $G_{T,\alpha}^{\chi}(t)$ defined in Eqs. (33) and (34), respectively, can be calculated using the residue theorem. The coefficients defined in Eqs. (35)–(38) can be given by

$$A_V(\epsilon, t) = -\frac{1}{2} \frac{\Gamma_L W}{(\epsilon - \tilde{\omega}_1)^2 (\epsilon - \tilde{\omega}_2)^2} - \frac{\Gamma_L W}{2} \sum_i \sum_{j \neq i} \frac{e^{-i(\tilde{\omega}_i - \epsilon)t}}{\epsilon - \tilde{\omega}_i} \left[\frac{it}{(\tilde{\omega}_i - \tilde{\omega}_j)^2} + \frac{2}{(\tilde{\omega}_i - \tilde{\omega}_j)^3} - \frac{1}{(\tilde{\omega}_i - \tilde{\omega}_j)^2 (\epsilon - \tilde{\omega}_i)} \right], \tag{D1}$$

$$\begin{aligned}
B_{V,L}^0(\epsilon, t) &= \frac{e^{i(iW - \epsilon)t} \Gamma_L W}{(iW - \tilde{\omega}_1^*)(iW - \tilde{\omega}_2^*)(\epsilon - iW)} \left[\frac{\Gamma_L W}{4(iW - \tilde{\omega}_1^*)(iW - \tilde{\omega}_2^*)} + \frac{1}{2} \right] - \frac{\Gamma_L W}{(\epsilon - \tilde{\omega}_1^*)(\epsilon - \tilde{\omega}_2^*)(\epsilon - iW)} \\
&\times \left[\frac{\Gamma_L W}{4(\epsilon - \tilde{\omega}_1^*)(\epsilon - \tilde{\omega}_2^*)} + \frac{1}{2} \right] - \sum_i \sum_{j \neq i} \frac{e^{i(\tilde{\omega}_i^* - \epsilon)t} \Gamma_L W}{(\tilde{\omega}_i^* - \tilde{\omega}_j^*)(\tilde{\omega}_i^* - iW)(\epsilon - \tilde{\omega}_i^*)} \left[\frac{it}{4} \frac{\Gamma_L W}{\tilde{\omega}_i^* - \tilde{\omega}_j^*} + \frac{\Gamma_L W}{2(\tilde{\omega}_i^* - \tilde{\omega}_j^*)^2} \right. \\
&\left. + \frac{\Gamma_L W}{4(\tilde{\omega}_i^* - \tilde{\omega}_j^*)(\tilde{\omega}_i^* - iW)} - \frac{\Gamma_L W}{4(\tilde{\omega}_i^* - \tilde{\omega}_j^*)(\epsilon - \tilde{\omega}_i^*)} - \frac{1}{2} \right], \tag{D2}
\end{aligned}$$

$$\Sigma_V^{<,0}(\epsilon) = -i \frac{\Gamma_L W^2}{\epsilon^2 + W^2} \tilde{f}(\epsilon) \left[\frac{2\epsilon}{\epsilon^2 + W^2} + \frac{1 - \tilde{f}(\epsilon)}{T_0} \right], \tag{D3}$$

$$\Sigma_T^{<,0}(\epsilon) = -i \frac{\Gamma_L W^2}{\epsilon^2 + W^2} \tilde{f}(\epsilon) \frac{\epsilon[1 - \tilde{f}(\epsilon)]}{T_0^2}. \tag{D4}$$

The spectral functions $\tilde{A}(\epsilon, t)$ and $\tilde{B}_L^0(\epsilon, t)$ can be written as

$$\tilde{A}(\epsilon, t) = \tilde{G}^r(\epsilon) + \sum_i \sum_{j \neq i} \frac{(\tilde{\omega}_i + iW)e^{-i(\tilde{\omega}_i - \epsilon)t}}{(\tilde{\omega}_i - \tilde{\omega}_j)(\tilde{\omega}_i - \epsilon)}, \quad (\text{D5})$$

$$\tilde{B}_L^0(\epsilon, t) = \tilde{G}^a(\epsilon) \tilde{\Sigma}_L^{a,0}(\epsilon) + \sum_i \sum_{j \neq i} \frac{e^{i(\tilde{\omega}_i^* - \epsilon)t} \Gamma_L W}{2(\tilde{\omega}_i^* - \tilde{\omega}_j^*)(\tilde{\omega}_i^* - \epsilon)}. \quad (\text{D6})$$

The thermoelectric coefficients $G_{V,\alpha}^X(t)$ and $G_{T,\alpha}^X(t)$ can then be calculated using Eqs. (D1)–(D6).

-
- [1] J. Chen, M. A. Reed, A. M. Rawlett, and J. M. Tour, *Science* **286**, 1550 (1999).
- [2] C. Joachim, J. K. Gimzewski, and A. Aviram, *Nature (London)* **408**, 541 (2000).
- [3] J. R. Heath and M. A. Ratner, *Phys. Today* **56**, 43 (2003).
- [4] G. D. Mahan and L. M. Woods, *Phys. Rev. Lett.* **80**, 4016 (1998).
- [5] F. J. DiSalvo, *Science* **285**, 703 (1999).
- [6] A. Majumdar, *Science* **303**, 777 (2004).
- [7] Y. Dubi and M. Di Ventra, *Rev. Mod. Phys.* **83**, 131 (2011).
- [8] G. U. Sumanasekera, B. K. Pradhan, H. E. Romero, K. W. Adu, and P. C. Eklund, *Phys. Rev. Lett.* **89**, 166801 (2002).
- [9] B. Wang, J. Zhou, R. Yang, and B. Li, *New J. Phys.* **16**, 065018 (2014).
- [10] L. A. Zotti, M. Bürkle, F. Pauly, W. Lee, K. Kim, W. Jeong, Y. Asai, P. Reddy, and J. C. Cuevas, *New J. Phys.* **16**, 015004 (2014).
- [11] X. Chen, L. Zhang, and H. Guo, *Phys. Rev. B* **92**, 155427 (2015).
- [12] J. Li, B. Wang, F. Xu, Y. Wei, and J. Wang, *Phys. Rev. B* **93**, 195426 (2016).
- [13] P. N. Butcher, *J. Phys.: Condens. Matter* **2**, 4869 (1990).
- [14] U. Sivan and Y. Imry, *Phys. Rev. B* **33**, 551 (1986).
- [15] Y. Zhu, J. Maciejko, T. Ji, H. Guo, and J. Wang, *Phys. Rev. B* **71**, 075317 (2005).
- [16] J. Maciejko, J. Wang, and H. Guo, *Phys. Rev. B* **74**, 085324 (2006).
- [17] Y. Xing, B. Wang, and J. Wang, *Phys. Rev. B* **82**, 205112 (2010).
- [18] L. Zhang, Y. Xing, and J. Wang, *Phys. Rev. B* **86**, 155438 (2012).
- [19] Z. Yu, L. Zhang, Y. Xing, and J. Wang, *Phys. Rev. B* **90**, 115428 (2014).
- [20] G. Tang, Z. Yu, and J. Wang, *New J. Phys.* **19**, 083007 (2017).
- [21] B. Wang, Y. Xing, L. Zhang, and J. Wang, *Phys. Rev. B* **81**, 121103(R) (2010).
- [22] L. Zhang, J. Chen, and J. Wang, *Phys. Rev. B* **87**, 205401 (2013).
- [23] G. Stefanucci and C.-O. Almbladh, *Phys. Rev. B* **69**, 195318 (2004).
- [24] G. Stefanucci, S. Kurth, A. Rubio, and E. K. U. Gross, *Phys. Rev. B* **77**, 075339 (2008).
- [25] X.-Q. Li, J. Y. Luo, Y.-G. Yang, P. Cui, and Y. J. Yan, *Phys. Rev. B* **71**, 205304 (2005).
- [26] X.-Q. Li and Y. J. Yan, *Phys. Rev. B* **75**, 075114 (2007).
- [27] H.-N. Xiong, W.-M. Zhang, X. Wang, and M.-H. Wu, *Phys. Rev. A* **82**, 012105 (2010).
- [28] J. Jin, M. W.-Y. Tu, W.-M. Zhang, and Y. Yan, *New J. Phys.* **12**, 083013 (2010).
- [29] M. Cini, *Phys. Rev. B* **22**, 5887 (1980).
- [30] A. Crépieux, F. Šimkovic, B. Cambon, and F. Michelini, *Phys. Rev. B* **83**, 153417 (2011).
- [31] A.-M. Daré and P. Lombardo, *Phys. Rev. B* **93**, 035303 (2016).
- [32] Z. Yu, G.-M. Tang, and J. Wang, *Phys. Rev. B* **93**, 195419 (2016).
- [33] F. Covito, F. G. Eich, R. Tuovinen, M. A. Sentef, and A. Rubio, *J. Chem. Theory Comput.* **14**, 2495 (2018).
- [34] C. Caroli, R. Combescot, P. Nozieres, and D. Saint-James, *J. Phys. C: Solid State Phys.* **4**, 916 (1971).
- [35] C. Caroli, R. Combescot, D. Lederer, P. Nozieres, and D. Saint-James, *J. Phys. C: Solid State Phys.* **4**, 2598 (1971).
- [36] M. M. Odashima and C. H. Lewenkopf, *Phys. Rev. B* **95**, 104301 (2017).
- [37] M. Ridley and R. Tuovinen, *J. Low Temp. Phys.* **191**, 380 (2018).
- [38] F. G. Eich, A. Principi, M. Di Ventra, and G. Vignale, *Phys. Rev. B* **90**, 115116 (2014).
- [39] F. G. Eich, M. Di Ventra, and G. Vignale, *Phys. Rev. B* **93**, 134309 (2016).
- [40] Č. Lozej and T. Rejec, *Phys. Rev. B* **98**, 075427 (2018).
- [41] E. C. Cuansing and J.-S. Wang, *Phys. Rev. B* **81**, 052302 (2010).
- [42] R. Tuovinen, N. Säkkinen, D. Karlsson, G. Stefanucci, and R. van Leeuwen, *Phys. Rev. B* **93**, 214301 (2016).
- [43] A. K. Slimane, P. Reck, and G. Fleury, *Phys. Rev. B* **101**, 235413 (2020).
- [44] N. S. Wingreen, A.-P. Jauho, and Y. Meir, *Phys. Rev. B* **48**, 8487 (1993).
- [45] A.-P. Jauho, N. S. Wingreen, and Y. Meir, *Phys. Rev. B* **50**, 5528 (1994).
- [46] H. Haug and A.-P. Jauho, *Quantum Kinetics in Transport and Optics of Semiconductors* (Springer-Verlag, Berlin, 1998).
- [47] G. Stefanucci, *Phys. Rev. B* **75**, 195115 (2007).
- [48] Y. Blanter and M. Büttiker, *Phys. Rep.* **336**, 1 (2000).
- [49] M. Ridley, A. MacKinnon, and L. Kantorovich, *Phys. Rev. B* **95**, 165440 (2017).
- [50] G.-M. Tang and J. Wang, *Phys. Rev. B* **90**, 195422 (2014).
- [51] M. Ridley, M. Galperin, E. Gull, and G. Cohen, *Phys. Rev. B* **100**, 165127 (2019).
- [52] Y. Wei, B. Wang, J. Wang, and H. Guo, *Phys. Rev. B* **60**, 16900 (1999).
- [53] Z. Feng, J. Maciejko, J. Wang, and H. Guo, *Phys. Rev. B* **77**, 075302 (2008).
- [54] M. P. Anantram and S. Datta, *Phys. Rev. B* **51**, 7632 (1995).
- [55] B. Wang, J. Wang, and H. Guo, *Phys. Rev. Lett.* **82**, 398 (1999).
- [56] J. Chen, M. ShangGuan, and J. Wang, *New J. Phys.* **17**, 053034 (2015).